

The International Journal of Robotics Research

<http://ijr.sagepub.com>

Collective Actuation

Jason Campbell and Padmanabhan Pillai
The International Journal of Robotics Research 2008; 27; 299
DOI: 10.1177/0278364907085561

The online version of this article can be found at:
<http://ijr.sagepub.com/cgi/content/abstract/27/3-4/299>

Published by:

 SAGE Publications

<http://www.sagepublications.com>

On behalf of:



Multimedia Archives

Additional services and information for *The International Journal of Robotics Research* can be found at:

Email Alerts: <http://ijr.sagepub.com/cgi/alerts>

Subscriptions: <http://ijr.sagepub.com/subscriptions>

Reprints: <http://www.sagepub.com/journalsReprints.nav>

Permissions: <http://www.sagepub.com/journalsPermissions.nav>

Citations (this article cites 5 articles hosted on the SAGE Journals Online and HighWire Press platforms):
<http://ijr.sagepub.com/cgi/content/refs/27/3-4/299>

Jason Campbell Padmanabhan Pillai

Intel Research
4720 Forbes Avenue
Suite 410, Pittsburgh, PA
15213 USA
{jason.d.campbell, padmanabhan.s.pillai}@intel.com

Collective Actuation

Abstract

Modular robot designers confront inherent tradeoffs between size and power. Smaller, more numerous modules increase the adaptability of a given volume or mass of robot, allowing the aggregate robot to take on a wider variety of configurations, but do so at a cost of reducing the power and complexity budget of each module. Fewer, larger modules can incorporate more powerful actuators and stronger hinges, but at a cost of overspecializing the resulting robot in favor of corresponding uses. In this paper we describe a technique for coordinating the efforts of many tiny modules to achieve forces and movements larger than those possible for individual modules. In a broad sense, our work aims to make actuator capacity and range at least partly fungible by algorithm design and ensemble topology, rather than being immutable properties of a particular module design. An important aspect of this technique is its ability to bend complex and large-scale structures and to realize the equivalent of large-scale joints. By enabling scalable joints, and the “muscles” that could actuate larger structures, our work makes it more likely that modular robot ensembles can successfully be scaled up in number and down in size.

KEY WORDS—cellular and modular robotics

1. Introduction

In principle, a modular, self-reconfigurable robot (MRR) may change shape, locomotion style or end-effector design based on local environmental conditions and goals. However, that flexibility can be severely constrained in the absence of scalable joints, bendable multi-module structures and the ability to exert forces greater than a single module’s actuation capacity. Work on chain-style MRRs (Yim 1993, 1994; Murata et

al. 1994, 2002; Yim et al. 2000) has relied upon the hinges and actuators in individual modules to form and bend joints and hence develop forces/torques proportional to the scale of the modules. Current work in lattice-style MRRs achieves self-reconfiguration by shifting modules across the surface of an ensemble (Rus and Vona 1999), by moving holes around within the ensemble (De Rosa et al. 2006) or via interpenetrating metamodules (Vassilvitskii, et al. 2002a,b). With some exceptions (e.g., Yim et al. (2001)), movement techniques for chain-style and lattice-style MRRs have been unable to generate forces larger than those possible from pairwise module interactions, a major limitation for large-scale systems with thousands to millions of modules.

Motivated by the very large MRR ensembles envisioned by Claytronics (Goldstein et al. 2005), we have developed a class of reconfiguration techniques that can be used to build flexible structures, compound joints and “muscles” which can combine the efforts of many modules to develop large forces and large ranges of motion. Our approach, which we call *collective actuation* (CA) (Campbell and Pillai 2006), is best suited to cellular, lattice-based modular robots with curved module shapes or rolling inter-module actuation modes such as those described by Goldstein et al. (2005) and Jorgensen et al. (2004) and becomes increasingly attractive as individual modules shrink. Collective actuation offers an added benefit of facilitating smooth shape changes (i.e. continuous or near-continuous bending and contouring), even in compact, lattice-based ensembles that would previously have been regarded as modifiable only by adding or subtracting modules from the surface of the shape.

Our work is part of the Claytronics project, a broad effort to develop hardware and software techniques for modular robot ensembles scalable to tens of millions of sub-millimeter modules. The vision behind the project aims at relatively unusual applications such as 3D visualization, self-reconfigurable antennas, telepresence and new forms of user interface. Unlike some other applications proposed for MRRs involving dozens to hundreds of modules (e.g. search and rescue, space exploration), these applications will need greater ranges of motion

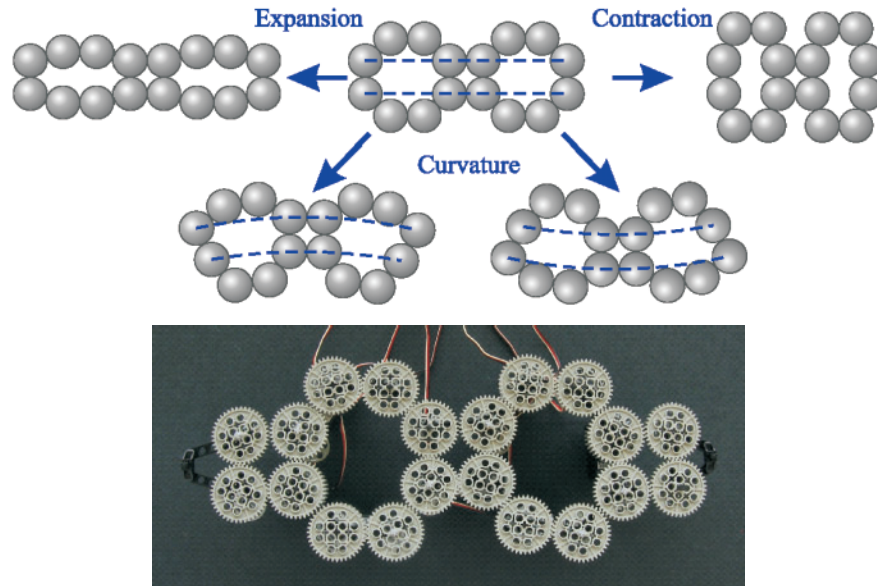


Fig. 1. One instance of a collective actuation system, consisting of two *octagonal cells* (see Figure 2 for cell definitions). Note that the physical prototype (bottom) includes four additional modules on each end to simplify the servomotor mounting arrangements.

(hundreds of module radii or more), larger relative forces and flexible structures to effectively reconfigure such fine-grained ensembles (10^4 – 10^8 modules).

An example of a collective actuation configuration, and a prototype used for approximating it physically, is shown in Figure 1.

1.1. Related Work

In the closest work to CA, Yim et al. (2001) describe an approach for exploiting singularities with chain-style modular robots. Their technique “ratchets” around such a singularity, using redundancy in a closed chain to repeatedly reposition the ensemble to do more work at high mechanical advantage. Joint locking mechanisms or brakes are required. Our work also exploits singularities for mechanical advantage, but focuses on a very different MRR domain involving (1) the rolling motion of modules rather than revolute joints, (2) external-field-based actuators rather than servomotors and (3) dense lattice-style ensembles rather typically sparse chain-style MRRs.

CA is also loosely related to parallel manipulators such as Stewart/Gough platforms (Gough 1956) and distributed manipulators such as distributed actuator arrays (Luntz and Messner 1995; Yim et al. 2000), both of which combine forces from several actuators to move a load or end-effector. Unlike distributed manipulators, an ensemble using CA can aggregate forces internally to rapidly self-reconfigure. CA also builds on a different set of mechanisms: the rotation of one module around

another rather than the linear actuators typical in parallel manipulators or the wheeled or more exotic manipulation techniques (e.g. air jets) utilized in actuator arrays.

Closed chains for manipulation have received extensive study (Lenhart and Whitesides 1994; Trinkle and Milgram 2002), including regarding the use of singularities to provide mechanical advantage (Kieffer and Lenarcic 1994). CA cells can be analyzed using the same tools (e.g. Jacobian nullspaces), although the cells we describe in this paper are simple enough to treat directly. Also, much work in analyzing closed chains applies manipulator redundancy to achieve a secondary goal (e.g. obstacle avoidance, controllability enhancement), whereas in many CA cells constraints (e.g. zero-slip, adjacent-cell coordination) leave no redundancy.

CA is also similar to loop or “rolling track” locomotion methods for chain-style modular robots, where closed rings of 10 or more modules roll across the ground, usually achieving relatively high speeds and efficiency relative to other modular robot gaits (Murata et al. 1994; Yim 1994). However, unlike a locomotion loop, a loop structure in CA is often merely one component of a more complex, flexible topology and CA is concerned more with *lifting* forces than with *driving* forces (thus CA configurations use smaller loops and aggregate them into structures).

Finally, Christensen et al. (2006) have recently demonstrated and characterized “muscles” implemented with ATRON modules. This work takes advantage of the rotational axis available within the ATRON module to allow chains of modules to generate forces over much longer distances than would be possible for individual units. The technique fits well

within the outline of what we have termed CA, albeit via a different mechanism from our own work owing to the differing module structure and capabilities for ATRON versus Claytronics.

2. Concepts and Definitions

2.1. Suitable Modular Robot Designs

We begin with an assumption that the robot modules used are spherical or highly faceted and capable of powered self-reconfiguration effected by rolling across each other's surfaces. An example of such modules is the pair of "catom" MRR prototypes described by Kirby et al. (2005).

MRRs can be modeled as complex machines and subjected to static and dynamic force analysis. In this paper we focus on an idealized model for such a modular robot machine with rolling parts and force-at-a-distance actuators arranged around the perimeter of each module (see Section 3). Non-convexities or asymmetries preclude our technique only insofar as they impede rolling. Our proposed approach does not apply to modules designed to dock/undock via pure translation and insertion (e.g. Suh et al. (2002)). Unfortunately, this last condition excludes many previously published MRR designs that emphasize bond rigidity over reconfiguration speed and flexibility.

2.2. CA Cells

A *CA cell* is a physically connected set of modules (i.e. a specialized class of metamodules) which can engage in coordinated motion to change the size, shape or aspect ratio of its perimeter. By changing its aspect ratio on command, a CA cell becomes something like a muscle fiber for modular robots, able to be combined with other cells (other muscle fibers) to construct aggregate "muscles" able to apply large forces to portions of the ensemble and its perimeter. However, in contrast to a muscle fiber or fixed mechanism the function of a CA cell will generally depend as much upon its actuation plan (algorithm) as upon the design of its mechanisms (hardware).

In this paper we investigate cells that are convex polygons constructed of closed chains of robot modules (Figure 2). These configurations offer more straightforward analysis and appear to be easier to implement physically than open-chain-based configurations. The symmetry of these configurations can also allow high-torque loads in mechanically disadvantageous positions to be borne via inter-module adhesion forces rather than as inter-module torques.

A CA cell operates by means of an *actuation plan*, an algorithm that describes which modules should rotate and at what relative speeds. Several actuation plans may be possible for a given physical configuration of modules, and in general these

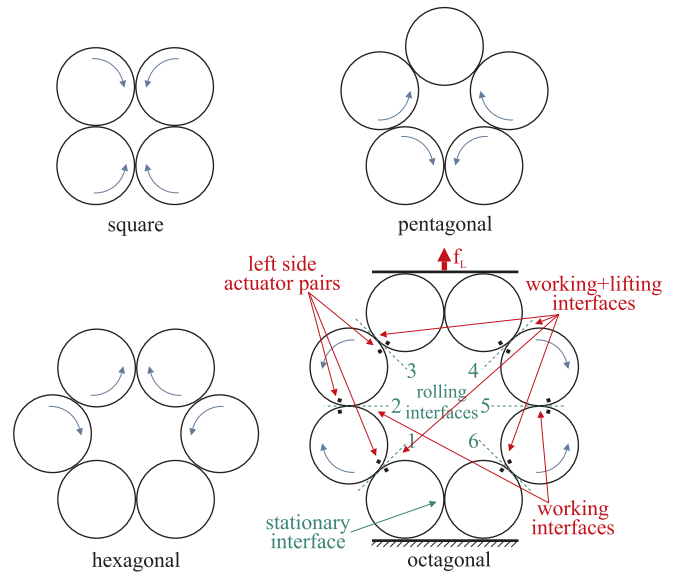


Fig. 2. Example CA cells. Lifting interfaces change the cell's aspect ratio by changing angle as they roll. Working interfaces contribute force to move the cell. f_L is the lifting force of the cell, as defined in Section 3.2.

plans will offer different results in terms of changing the cell perimeter.

CA cells may exist in two dimensions as well as in three. We limit our discussion here to the 2D case as this simplifies the analysis, diagrams and explanations involved. However, we believe that the techniques we introduce extend to three dimensions and plan to detail that extension in future work.

We call the physical intersection between a pair of modules an *interface*, and classify interfaces into *rolling interfaces* and *stationary interfaces* for a given cell configuration and actuation plan. We further identify rolling interfaces which are *lifting interfaces*, in which the angle between two modules changes during a given actuation plan, and *working interfaces*, which power motion of the cell with their actuators. Examples of these cases can be seen in Figure 2.

2.2.1. Combining Cells for Scaling and Control

The capacity or range of motion of an actuation cell can be extended by placing multiple cells next to one another. For instance, putting two cells side by side can in general double the potential force with which the joint system acts, and stacking two cells can in general double the range of motion over which the conglomerate can move. Neighboring actuation cells may also add degrees of control freedom in the resulting structure. Such an added degree of freedom might be the ability to form a slanted or curved surface from an otherwise flat plane

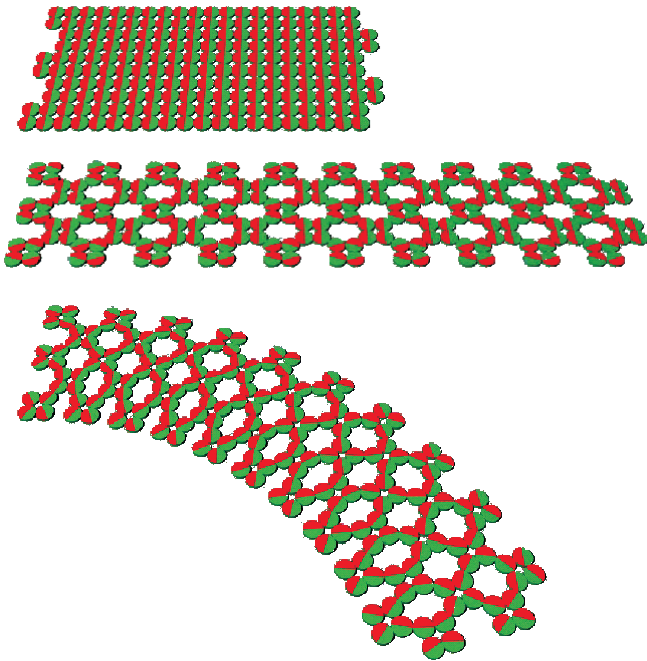


Fig. 3. Stretching and bending a structure composed of octagonal CA cells. No slip between modules is involved. Shading serves to illustrate rotation. Note that the maximum length variation possible for octagonal cells is 100% from the fully compressed state, and that at both full extension and full compression curvature is zero. (However, with even a small deviation from full extension or compression very significant curvature is possible.)

of modules, or the ability to bend a cantilever composed of many modules (as in Figure 3).

Adjoining CA cells can meet at pairs of stationary modules or at pairs of rolling modules. In the latter case the two actuation plans for the cells involved must call for equal speeds and opposite directions of rotation in the modules being joined, which can prevent multiple-cell structures from offering additional degrees of freedom. Hence, in situations where curved or bending structures are desirable cells with larger numbers of stationary modules (e.g. octagonal, rather than hexagonal or pentagonal) are preferable.

2.2.2. Advantages of Hierarchical Decomposition

Although it is possible to imagine a CA cell composed of an arbitrarily large number of modules, there are analytical and practical reasons for keeping CA cells small and assembling those cells into larger multi-cellular structures. First, the analysis of smaller cells is easier to carry out. Second, identifying particular repeated parts (e.g. CA cells) whose relationships hold locally enforced invariant relationships can substantially

simplify configuration planning and design. Third, the implementation of reconfiguration and motion will generally require tight coordination of the relative speeds of motion within a cell, and coordination complexity and latency grows rapidly with the number of participants.

In general, a CA cell will offer fewer degrees of freedom via its parameters (size, shape, aspect ratio, curvature, etc.) than the number of module–module interfaces involved. This reduction in degrees of freedom results from the cell enforcing particular internal relationships between its constituent modules. As such internal constraints can be maintained via local communication within the cell itself, and because the higher-level characteristics associated with the cell can be expressed more compactly than the total set of module poses, *CA can substantially reduce the “wide-area” bandwidth needed for planning or controlling a large modular robot.* (By “wide area” we mean messages traveling further than a few modules.)

In many cases the control parameters for a cell can be specified in a scale-invariant manner: for instance, a cell’s perimeter may be described in idealized form as a parallelogram or set of Bezier curves. Adjacent cells using compatible representations to describe their perimeters can be coupled to implement a single perimeter definition across all (i.e. the overall shape of two parallelograms can, with some loss in internal freedom, be described as a larger parallelogram). This can lead to a further reduction in implementation and planning complexity, and simplify ensemble control.

2.3. Performance Criteria and Figures of Merit

There are four major cell performance criteria about which we are concerned:

- (1) force;
- (2) distance moved;
- (3) aspect ratio range;
- (4) degree of curvature possible.

These characteristics can vary both based on the geometric configuration of the modules in the cell and on the actuation plan(s) utilized. Also, while the distance moved (2) and degree of curvature (4) can be expressed as scalars and the aspect ratio (3) as a pair of scalars, force (1) will generally be contingent upon one or more continuous angle measures which vary as the cell moves. Thus, we should consider the *force profile* for each cell, meaning the evolution of force over time as the cell goes from one extreme to another, as well as of the maximum and minimum mechanical advantage realized. In each case we can speak in terms relative to other points on the force profile, or, with suitable parameters, assumptions or tests, we can speak of the forces in absolute terms.

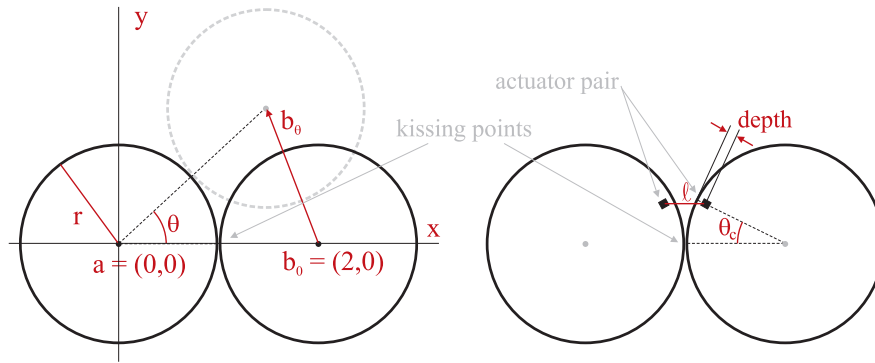


Fig. 4. Parameter definitions for a rolling modular robot system consisting of modules a and b in mutual contact, using force-at-a-distance actuators of known depth to drive a rolling motion described by angle θ .

The distance moved is expressed as a percentage: the increase in size of the maximally expanded (largest) configuration from the maximally compressed (smallest) configuration of the cell. For example, if a cell can be compressed to be as short as four module diameters in height and can be expanded to as tall as six module diameters we say that the cell's distance moved figure is $(6 - 4)/4 = 2/4 = 50\%$.

The aspect ratio range is expressed as a pair of scalars, each reflecting the cell's height/width, where one of the scalars is the minimum and the other the maximum given the cell's full range of motion as measured on a chosen pair of height/width axes.

The degree of curvature will be measured in terms of the radius of the outside edge of the curved shape, normalized to the module radius.

3. Analysis

3.1. Module-on-module Rolling Model

Robot modules based on rolling motion across curved surfaces are likely to employ some form of force-at-a-distance actuation, i.e. magnetic or electric fields. The catom modules described by Kirby et al. (2005), for instance, self-reconfigure using (opposite polarity) electromagnets on adjacent modules. By progressively energizing a sequence of electromagnets spaced around the perimeter of each cylindrical module a rolling motion results. For this paper we generalize this actuation model as follows. Given two cylindrical modules a and b (see Figure 4), each of radius r , angular (rolling) position θ , with module a centered at the origin, the location of module b 's center can be expressed as follows:

$$b = \begin{bmatrix} 2r \cos \theta \\ 2r \sin \theta \end{bmatrix} \quad \frac{db}{d\theta} = \begin{bmatrix} -2r \sin \theta \\ 2r \cos \theta \end{bmatrix}. \quad (1)$$

For point actuators on the surface of b , the geometry of those points' motion relative to counterpart points on a is described by an epicycloid. In the more general case where the actuators lie at a depth d beneath the surface, the motion is instead described by an epitrochoid (see Figure 5). Given that two actuators are at an equal angle ϕ from the kissing points of the cylinders, the relationship ℓ between the actuator on b and its counterpart on a is given by the vector:

$$\begin{aligned} \ell &= \begin{bmatrix} (1-d)r - 2r \cos \phi + (1-d)r \cos 2\phi \\ -2r \sin \phi + (1-d)r \sin 2\phi \end{bmatrix} \\ &= \begin{bmatrix} -2r(\cos \phi)(1 + (d-1) \cos \phi) \\ -2r(1 + (d-1) \cos \phi) \sin \phi \end{bmatrix}. \end{aligned} \quad (2)$$

When viewed as a scalar distance $|\ell|$, this yields a simple sinusoid (3). If the actuators are not at an equal angle from the kissing points, i.e. they are out of "phase" with each other, the distance versus angle curve becomes more complex (see Figure 6). While minor misalignments (under 10°) have little impact on actuator forces, larger phase mismatches can substantially weaken actuation:

$$|\ell| = 2r + (2rd - 2r) \cos \phi, \quad (3)$$

$$\frac{d|\ell|}{d\phi} = 2r(1-d) \sin \phi. \quad (4)$$

Considering the angle ϕ between the actuators and the kissing point, and the position of the kissing point governed by the rotation angle θ , we can relate ϕ to θ with the formula $\phi = \theta_c - \theta$. Here, θ_c indicates the angular position where the actuators reach the closest approach, i.e. on the line joining the modules' centers and the kissing point. At this point $\phi = 0$. Combining this observation with (1) and (4) we see that changes in the

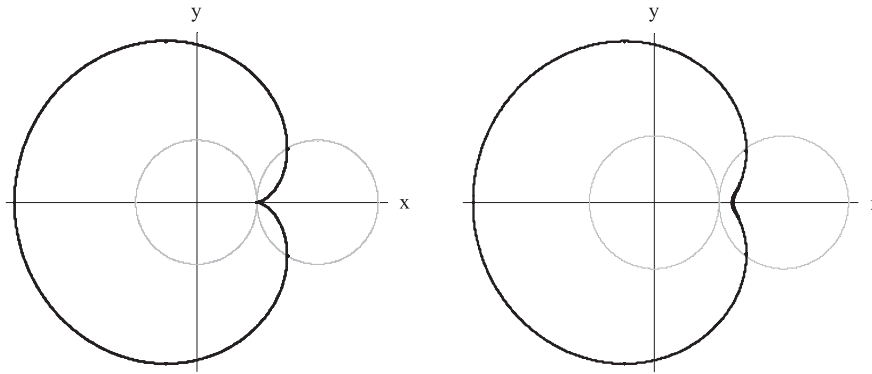


Fig. 5. (a) Epicycloid path for an actuator at zero depth and (b) epitrochoid path for an actuator slightly sunken into the module. For each plot, θ varies from 0 to 2π and $\theta_c = 0$ as defined in the text. The dark circuit shows the path traced by a given actuator during a single full rotation of the module on the right around the module on the left.

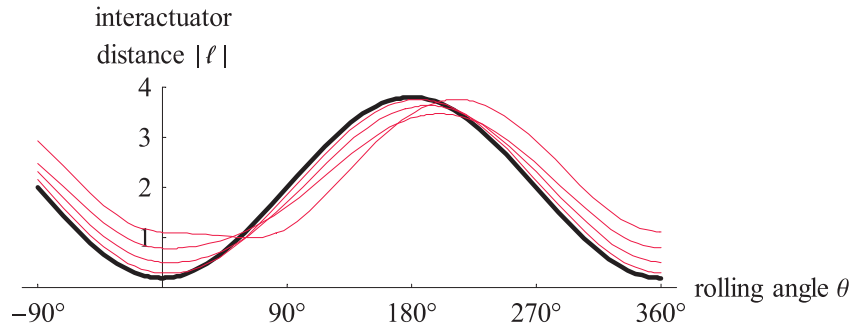


Fig. 6. Distance between actuators for a two-catom system of radius = 1 and actuator depth = 5% of radius. The bold curve reflects perfect phase matching. The thinner curves show 10°, 20°, 30° and 90° phase mismatch. Phase mismatches reduce actuator force.

distance $|l|$ between a given pair of actuators will relate to the change in relative position b of the moving cylinder’s center as follows:

$$\begin{aligned} \frac{db}{d|l|} &= \frac{db}{d\theta} \cdot \frac{d\theta}{d|l|} \\ &= \begin{bmatrix} -2r \sin \theta \\ 2r \cos \theta \end{bmatrix} \cdot \frac{1}{2r(1-d) \sin(\theta_c - \theta)} \\ &= \frac{\csc(\theta_c - \theta)}{d-1} \begin{bmatrix} \sin \theta \\ -\cos \theta \end{bmatrix}. \end{aligned} \tag{5}$$

This expresses the effective “lever arm” through which attraction between two actuators works to move the center of cylinder b .

The magnitude of action-at-a-distance forces, such as those affected by magnetic and electric fields, diminishes with distance. In this paper we simplify that relationship to an inverse-square law. For an electromagnet approximated by a simple solenoid via the Biot–Savart law we obtain the field strength as proportional to $1/(r^2 + R^2)^{1.5}$ in the near-field region, where R is the radius of the coil and r is the scalar distance to the point where the field is measured. For moderate coil radii this approximation works well, but is overly optimistic in the near field (inside 0.2 module radii) for coils close to their maximum size based on module radius and number of actuators. Electric fields, described by Coulomb’s law, are explicitly governed by an inverse-square relationship with distance.

Combining the differential motion result (5) with an approximation for actuator force roll-off ($f = f_m/\text{distance}^n$), we can define a vector force quotient q expressing both the direction and potential mechanical advantage in which a force exerted by the actuators will bear upon module position b :

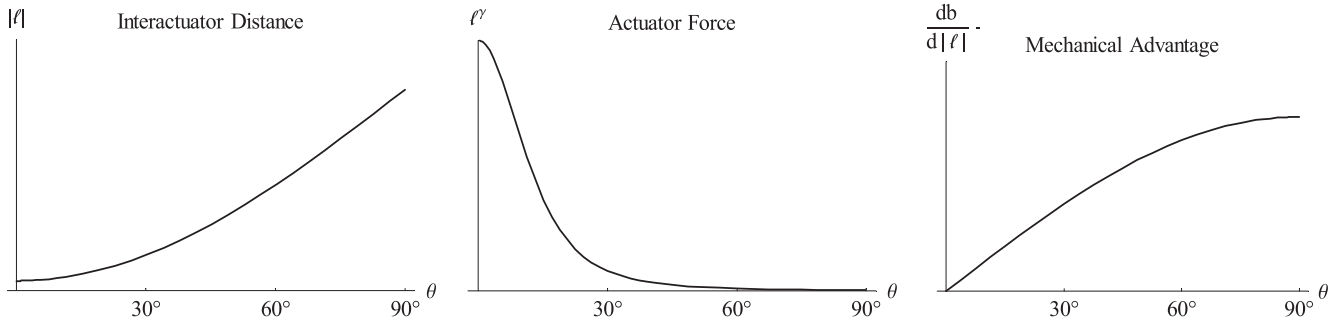


Fig. 7. Evolution of the distance between a pair of actuators, actuator force magnitude (assuming an inverse-square law) and raw mechanical advantage as one catom rolls around another. 0° is the point of closest approach for the pair of actuators.

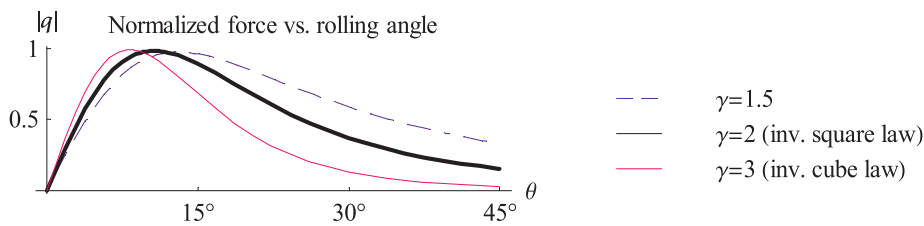


Fig. 8. Force versus angle curves for different force/distance law exponents. This is the result of combining the effects of actuator force fall-off and mechanical advantage increase shown in Figure 7. Each curve here shows the impact of a particular force/distance law for the actuators: inverse cube $\gamma = 3$ (thin curve), inverse square $\gamma = 2$ (thick curve), “ $n \log n$ ” $\gamma = 1.5$ (dashed curve) with $d = 5\%$ of catom radius and $\theta_c = 0$. The peaks are at 13° , 10.7° and 8.3° .

$$\begin{aligned}
 q &= \frac{db}{d|l|} \ell^\gamma \\
 &= \frac{\csc(\theta_c - \theta)(2r - (2r - 2d) \cos(\theta - \theta_c))^\gamma}{d - 1} \cdot \begin{bmatrix} \sin \theta \\ -\cos \theta \end{bmatrix}.
 \end{aligned}
 \tag{6}$$

Plotting the reciprocal of the norm of q for varying θ (see Figure 8) allows us to see that, even before considering the direction or absolute magnitude of work (e.g. projection onto the gravity vector, etc.), the effectiveness of a given actuator peaks a short distance from the kissing point. This distance is only mildly influenced by the exponent in the force distance law. The peak is due to the opposing effects of increasing lever arm and decreasing actuator force during rolling motion away from the actuator kissing point. The location of this peak is an important design and control consideration, and is independent of the physical scale of the modules.

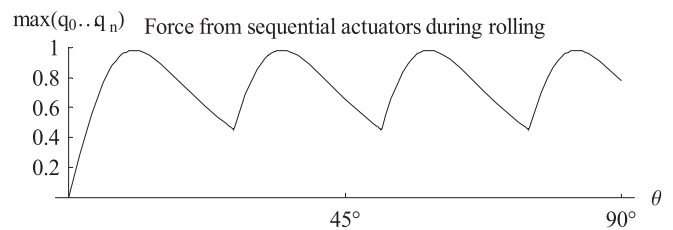


Fig. 9. Relative force available to drive a rolling catom, as generated by constant excitation in a series of $n = 15$ electromagnetic actuators spaced at 24° intervals along the rolling and stationary catoms’ surfaces. The magnet depth $d = 5\%$.

3.1.1. Sequences of actuators

A practical spherical or cylindrical robot module will necessarily include multiple actuators around its perimeter. When multiple actuators are used in sequence to drive rolling motion, the resulting force curve will be a composition of the individual force curves (see Figure 9). The “duty cycle” or average force value of this composite curve will depend on the density at which actuators are spaced, thus reflecting the benefit of being able to operate each actuator closer to its peak force region.

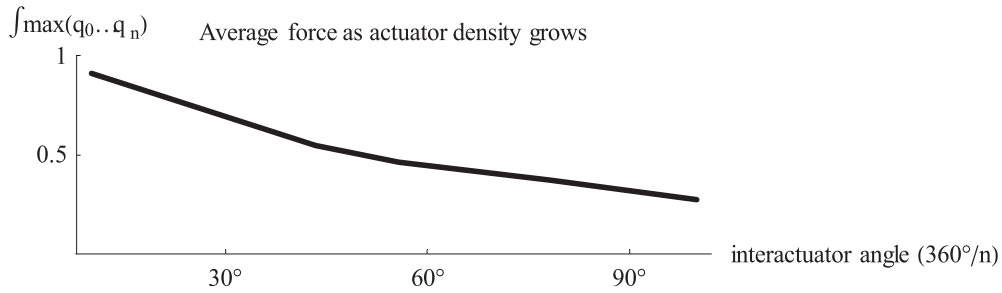


Fig. 10. Multiple-actuator “duty cycle” versus actuator spacing. This plot captures the relationship between average force available and total number of actuators total around a circle (1/angle). Each datapoint is integrated over 180° and the inverse-square law is assumed.

Figure 10 illustrates the relationship between actuator spacing and average force. (For spherical modules actuator spacing may be less regular than for cylindrical modules because so many different axes of rotation are possible and the placement of actuators will be limited by weight, complexity and engineering concerns.)

3.2. Multi-module System (Cell) Dynamical Analysis

Consider the octagonal cell shown earlier (Figure 2). Suppose that the catoms indicated with arrows initiate rolling motion in the directions shown. For the eight catoms, a total of six pairs of actuators will be involved in powering the motion (at the three inter-catom interfaces around the rolling catoms on each side of the figure). With infinite friction (zero slip) any one of the three pairs of actuators on each side will suffice to cause rolling motion on all three interfaces. We call such an arrangement *actuator entrainment*. Lifting of the cell is caused entirely by the change in angle along interfaces 1, 3, 4 and 6, and we call such interfaces *lifting interfaces*. By projecting Equation (6) in a vertical direction we can compute the lifting force along each of the working interfaces.

As the three actuator pairs on each side are entrained, that is, they are part of the same mechanical system, they act together to lift. The upper and lower working interfaces are symmetric, so we can treat them identically. The end result is that we can multiply the resulting lifting force from a single lifting interface by the number of working interfaces (i.e. those which contribute energy to moving the system) divided by the number of lifting interfaces (i.e. the distance over which the cell moves), in this case 3/2. Note that interfaces 2 and 5 (as shown in Figure 2) do contribute energy to moving the system as long as the zero-slip constraint is enforced by friction, gear teeth or some other mechanism. As the two sides of the cell act in parallel we again multiply the lifting force (now from a single side) by two to obtain the total lifting force:

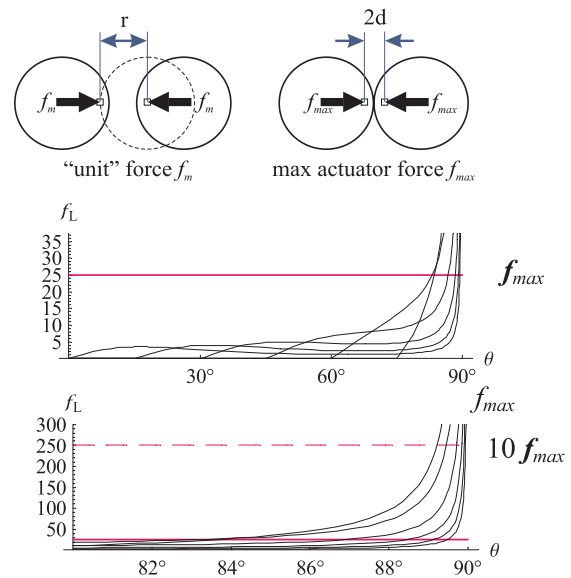


Fig. 11. Lifting force exerted by an octagonal collective actuation cell using actuators spaced at 15° intervals and a depth $d = 0.1$ (10% of one module radius). The solid line in the upper plot marks the point at which the lifting force is equal to f_{max} for a pair of actuators (see the text). The dashed line in the lower plot marks $10 \times f_{max}$.

$$f_L = 2 \left(\frac{3}{2} \right) \left(\frac{1}{q \cdot \begin{bmatrix} 0 \\ 1 \end{bmatrix}} \right) f_m = \frac{-3(d - 1) \cos \theta}{\csc(\theta_c - \theta)(2r - (2r - 2d) \cos(\theta - \theta_c))^2} f_m \quad (7)$$

Figure 11 plots f_L for one module rolling around another from a horizontal starting point up to a vertical position. The term f_m is the unit-distance actuator force: the force exerted by

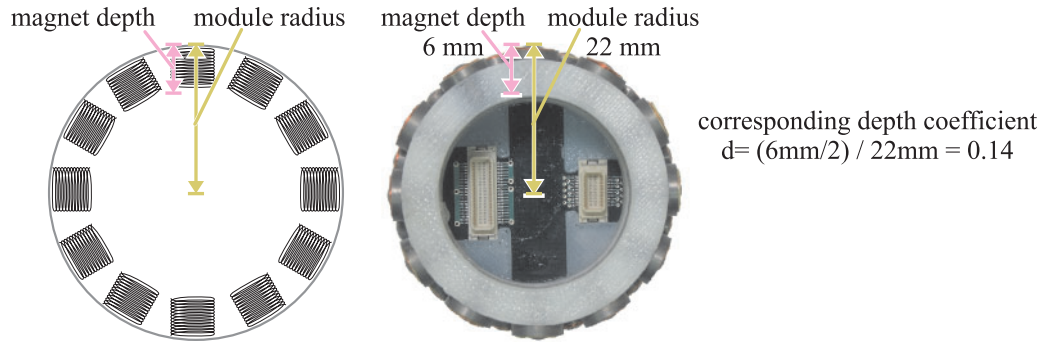


Fig. 12. Illustration of the magnet depth parameter d . The magnet ring on the right is from a catom module, with the ends of the magnets visibly protruding from a white plastic frame. Note that d for this magnet ring would be 0.14. Our analyses use a conservative value of $d = 0.1$, which somewhat understates the mechanical advantage possible using collective actuation with catoms. Larger values of d lead to an earlier crossover with f_{\max} in Figure 11.

one module on another when their actuators are one module radius apart. Given this relationship and d , the depth at of each actuator as a proportion of module radius, we can use (7) to obtain a comparative feel for the power of the lifting force in this CA cell. It is useful for this purpose to define f_{\max} , the maximum possible attractive force between two actuators at their point of closest approach, i.e. when $\theta = \theta_c$. Note that an f_{\max} force can never do useful lifting for an individual module since, by definition, f_{\max} only occurs when modules can be pulled no closer. The solid line (at a force of $25 f_m$) in the plots in Figure 11 shows the point at which the lifting force from the octagonal CA cell is equal to f_{\max} . The dashed line shows the point at which the lifting force is equal to $10 \times f_{\max}$.

For an electromagnet-based module, $d = 0.1$ likely understates the mechanical advantage of module rolling (and therefore of CA) because d is measured from the surface of the module to the *center* of the solenoid and real magnet coils would typically be larger than 0.2 module radii in size (see Figure 12). Larger values of d lead to an earlier crossover with f_{\max} . With careful geometry substantially larger lifting forces could be realized than with individual modules.

For an electric-field-based module, $d = 0.1$ may overstate the change in mechanical advantage possible because the actuators would likely be realized as plates on the surfaces of the modules.

Putting real units into this analysis is challenging in the absence of a complete module design (energy sources, actuators, control systems, exact geometry). Our approach here is intended to guide the module design process, in particular with regards to the tradeoff between more numerous, smaller actuators and fewer, larger ones. As we converge on specific sets of module design parameters it is then possible to use the same method to predict the forces involved in absolute terms.

3.3. Hierarchical Structures (Multiple Cells)

One benefit of the metamodule or cellular approach to CA is that it reduces ensemble control complexity. In particular, we can use cells as building blocks, stacking them together to form larger structures. By executing local controls in parallel at each cell, we can actuate the larger structure with a limited increase in control, message and planning complexity.

In the simplest case, there are two basic methods of stacking and operating multiple cells: in series (stacked on top of each other in the direction of actuation) and in parallel (placed next to each other). With the default control system in which all of the cells are actuated in the same manner, the simple series stacking results in a multiplication of actuation distance by the number of stacked cells. In terms of relative distance or percentage elongation, there is no difference from the single cell, although the absolute distance may be much longer. Likewise, there is no change in the force applied in the direction of work.

For the parallel case, cells work side by side at the same distance. However, the net force is multiplied by the number of parallel cells bearing the load. Combining both of these, a $k \times k$ array of cells produces the effects of both greater force and greater absolute range of motion. In three dimensions, an additional dimension of parallel cell placement is also possible.

A second benefit of multicellular structures is their ability to introduce useful additional degrees of freedom, at a very modest increase in control complexity. Varying cell actuation parameters through the structure can result in more complex shapes and some useful large-scale behaviors can be achieved with simple patterns of actuation repeated across the structure. For instance, the bending bar (shown in simulation in Figure 3, and as a physical prototype in Figures 1 and 20) employs a technique we call differential actuation, whereby the cells on either side of the bar are set to expand by different amounts to

achieve a desired curvature and length. To maintain structural integrity, this technique must also account for the variation in length required from top to bottom within each layer, as well as between layers. (Just as layers in a stone arch must vary in curvature across their thickness.) Despite those variations, the overall effect of the beam’s cellular structure is to dramatically reduce the control complexity of the total system.

3.4. Force/Weight and Structure Height

The above discussion on hierarchical control suggests that we can stack cells in an unlimited manner, but in practice actuator capacities will limit the height of the column that a cell can successfully lift. Our dimensionless analysis can be extended to analytically relate the force/weight ratio of a module to the maximum height of a column of CA cells.

If we assume that the octagonal cell used in our examples (see Figure 11) will be held at or above $\theta = 30^\circ$ then from (7) we can compute that the worst-case lifting force available from the cell will be $4.6 f_m$ or approximately $4.6/25 = 18.4\%$ of f_{max} . As f_{max} expresses the maximum force one module can exert upon another at zero distance, we can replace it with $f_{max} = Sw$, where S is the strength/weight ratio of one module actuator at minimum distance and w is the weight of a module. If we neglect the forces required for a cell to support itself, the weight supported by the lowermost cell in a column of h cells will be $8(h - 1)w$. If we solve for the minimum actuator force needed in that bottommost cell we arrive at

$$S = 43.5(h - 1). \tag{8}$$

Thus, our modules need a strength/weight ratio of 43.5 times the number of layers in the column we wish to support in order to prevent the bottommost cell from collapsing. Present modular robot prototypes do not display anywhere near these strengths; however, preliminary calculations our research group has conducted suggest that hollow, MEMS-produced $600 \mu\text{m}$ diameter cylindrical modules with surface electrostatic actuators could attain actuator strength/weight ratios of 10,000. Initial FEM simulations support this figure. This would permit a 230-layer tower of octagonal cells, corresponding to a column between 25 and 50 cm high.

Taller structures could come in one of several ways. First, by constraining cells to larger θ values (with correspondingly greater mechanical advantage), less actuator strength is needed and a column could be taller, although less able to change its size. For instance, at $\theta = 60^\circ$ a column could be between about 70 cm and 1 m high, and at $\theta = 85^\circ$ a column could reach 4.2 m. Second, taller structures would also be possible by allowing cells near the bottom of the column to collapse either into a denser, fixed structure: either the cubic packing natural to an octagonal cell (with some requirement to control the risk of instability) or into a tetrahedral HCP or FCC packing. Such strong, incompressible, but no longer flexible structures would be akin to bone in biological systems.

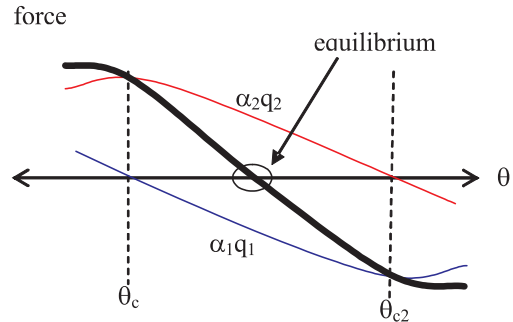


Fig. 13. Forces from two adjacent pairs of actuators, at θ_{c1} and θ_{c2} , and net resultant force as functions of the contact angle θ , based on Equation (6). Here, a positive force causes an increase in θ , while a negative force tends to decrease θ , so the net force will move the contact point to the equilibrium position. Adjusting scaling factors α_1 and α_2 between 0.0 and 1.0 will allow arbitrary placement of the equilibrium point between θ_{c1} and θ_{c2} . Note that the actuators are only used to generate attractive forces.

4. Control Algorithms

4.1. Local Control at an Interface

The motion model assumed in Section 3 requires an ability to roll one module continuously about another, but any real design will be limited to a discrete set of actuators. Positioning and holding the contact point between adjacent pairs of actuators requires careful control over both pairs of actuators. Observe from Equation (6) and Figure 8 that for contact positions near an actuator pair the actuator forces can be modeled linearly. Like a simple spring, force increases with displacement and is directed towards the equilibrium point. Using this property, for small actuator spacings (e.g. less than 10°), we can design an open-loop control strategy to position and hold the contact point anywhere between adjacent pairs of actuators. Assume that we have actuator 1 at θ_{c1} and adjacent actuator 2 at θ_{c2} on one module, as well as their counterparts on a second module. Assume further that we can attenuate the force from each actuator by factors α_1 and α_2 , each between 0.0 and 1.0 (for instance, via pulse-width modulation).

Applying Equation (6), we can find the net force from the two pairs of attenuated actuators as $\alpha_1 q_1 + \alpha_2 q_2$, as illustrated in Figure 13. The contact point will be the equilibrium point (where the forces sum to zero). For a desired θ between contacts (θ_{c1}, θ_{c2}), we can set this sum to zero and solve for a matching ratio α_1/α_2 . We can then pick absolute α values of 1.0, and some value between 0.0 and 1.0. Note that this mechanism cannot directly deal with overshoot or oscillation, and any damping must come from friction. Furthermore, this ignores the effects of external loads.

With the capability to sense the position of the contact point accurately we could also construct a closed-loop controller for the same purpose. As the actuator response for small displacements is very close to linear, a simple PID controller can servo the contact point to a desired position, damp oscillations and reduce steady-state error due to external loads. The desired force indicated by the controller can be equated to $\alpha_1 q_1 + \alpha_2 q_2$, to find a ratio α_1/α_2 , and α values selected as above. Finally, as this technique directly controls the net forces generated rather than relying on increasing restitution force with increasing displacement, this method permits operation at larger angular displacements (and larger actuator spacing), although at a cost of increasing divergence from the linearized region.

4.2. Coordination of Modules within a Cell

To maintain CA cell properties, it is necessary to ensure that all of the working interfaces operate in parallel, moving the contact points an equal amount over a given time interval. One way to limit the error between the different interfaces is to subdivide the desired actuation into smaller steps.

Given a starting configuration of the cell, we compute $\Delta\theta_b$, the angular distance that each interface b must roll to reach the desired target configuration. We divide actuation into k steps, advancing each interface b by $\Delta\theta_b/k$ at each step. The modules wait until all interfaces have reached the current actuation position before proceeding to the next step. As cells are small, tightly coupled units this can be implemented efficiently with simple synchronization primitives. The maximum angular error between interfaces will then be bounded by the largest $\Delta\theta_b/k$ value.

4.3. Control of Multi-cell Structures

Cells can be combined from larger actuation groups. For instance, octet cells can be stacked horizontally, vertically and in depth to form large rectilinear prisms that can change their aspect ratios (see Figure 14). For each cell, we can specify the desired cell configuration with a single parameter, β , which varies from 1.0 to 2.0, indicating the relative width of the cell. To actuate the prism, all of the member cells move in parallel to the same β value, with this target being communicated either through a distribution tree or simple flooding.

Owing to unequal external loads, some cells may be able to actuate faster than others. We can subdivide the actuation into many steps and coordinate these steps as in the intra-cell control outlined above. However, we need to ensure scalability and efficiency of the coordination employed, and barrier synchronization may be prohibitively costly in messaging terms for large ensembles. One possible solution is to use a decentralized, distributed mechanism to compute a consensus on the current step number and rate of execution. A local controller

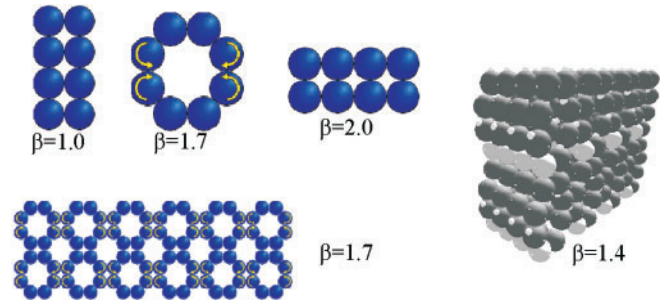


Fig. 14. Single and stacked octet cells, actuated to vary aspect ratios, as specified through parameter β .

on each module then adjusts local actuation step timing to track the consensus step number and rate.

In addition to rectilinear prisms that change aspect ratios, the octet cells can also form structures that can bend, as in Figure 15. Here, we have an $n \times m$ array of octet cells where the n layers of cells achieve a desired curvature, specified by φ . The modules at different layers (even within a cell) must rotate to a varying degree to reach the desired form without tearing the structure. Figure 15 derives the relationships between these rotations, given by ω_k values. Each block of four modules forming a square rotates an equal angular distance (i.e. modules share a common ω value); otherwise, slipping would occur or the block would tear.

The set of constraints leaves one degree of freedom: all of the modules can rotate in place, in opposing directions. That remaining degree of freedom can be eliminated by setting ω_0 to zero, corresponding to a fictitious layer of modules at the top. We can then search (e.g. binary search) for a value for ω_1 that will permit the generation of all of the remaining ω_k values without violating any constraints. Not all combinations of β and φ have valid solutions. Extreme values of β (1.0 or 2.0) cannot sustain any curvature, whereas intermediate values allow a range for φ .

5. Experiments

5.1. Rolling Modules using Magnetic Forces

Our colleagues in the Claytronics project have constructed several versions of cylindrical modules that utilize radially oriented electromagnets to self-reconfigure (see Figure 16 and also Goldstein et al. (2005) and Kirby et al. (2005) for further details). These modules demonstrate some of the principles involved in self-reconfiguring round shapes (cylinders and spheres). Unfortunately, the scale at which the modules are constructed (5 cm) precludes the force/mass ratio necessary for CA. Nonetheless, these robot modules show that self-reconfiguration via rotation is possible and illustrate the viability of techniques such as continuous rotation via staged energizing of point-force actuators.

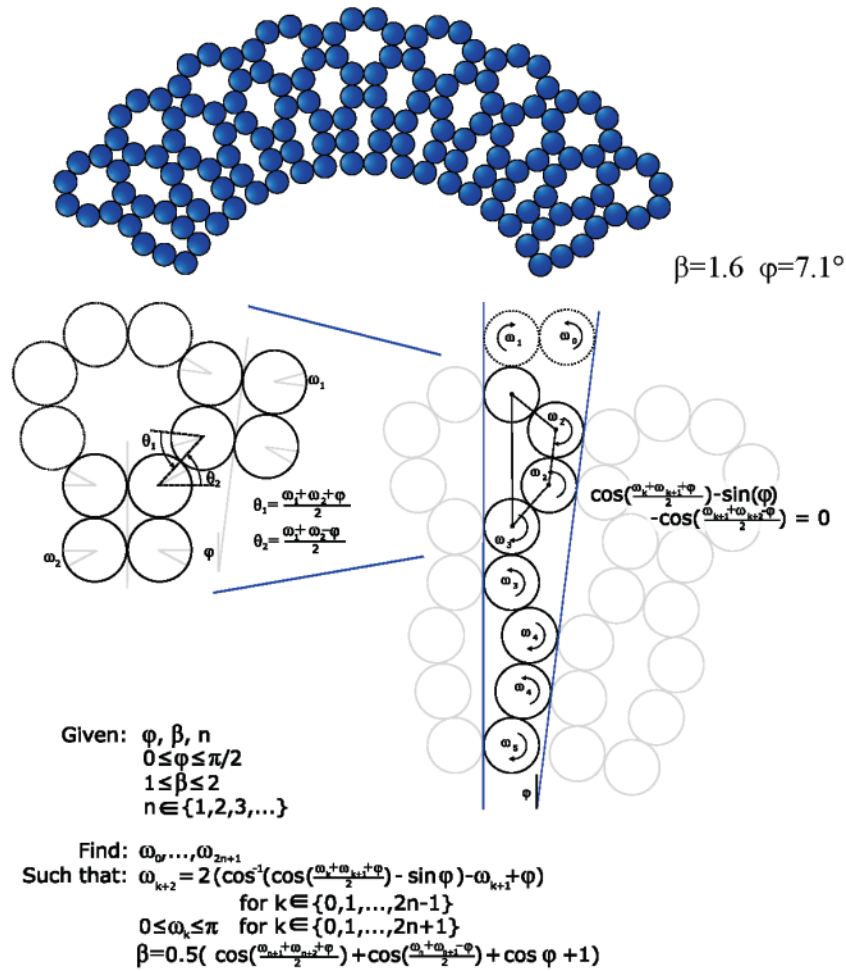


Fig. 15. Bending structures created from stacked octet cells. The structure is n cell layers thick (here $n = 2$). Here β specifies the desired width, φ specifies desired curvature, defined as the angle between the centerline of a cell and its side, ω_k indicates the angle to which modules at different layers must rotate with respect their neighbors and ω_0 is for a fictitious layer of modules introduced to make the generative formulation clearer, and can be set to an arbitrary value of zero. One can perform a binary search to then find ω_1 and generate the other ω_k values such that all of the constraints hold. Not all combinations of β and φ have solutions.

5.2. Self-articulating Structures

We showed earlier (Figure 3) a simulation of a variable-curvature beam constructed using a long set of octagonal CA cells. By controlling the aspect ratio and skew of each cell we could specify the aspect ratio and curvature of the overall beam. We have built a physical prototype of such a bending beam using 20 plastic gears and 8 servomotors under the control of a microcontroller (see Figure 17). While not replicating the force-at-a-distance actuation mechanism we eventually expect to use, this assembly has allowed us to study the performance of a real-world CA system.

We can determine the control angles in such a beam based on the desired extension, or relative width of the cells, and cur-

vature. The extension parameter (β) ranges from 1.0 to 2.0 for the octagonal cell used here. The curvature attainable depends on the extension, and Figure 18(a) plots the tightest possible curvature, expressed as the outside radius normalized to the module radius, for various extension values of the inner layer. The lines show results for beams composed of $2 \times n$, $3 \times n$ and $4 \times n$ arrays of cells. Although thicker beams restrict the tightness of the curvature attainable by bending, Figure 18(b) shows that when normalized for thickness (in number of cell layers), the results are nearly identical. Thus, bending actuation can scale to larger structures. We also determine the maximum range of motion of one end of such a beam structure when the other end is fixed. Figure 19 shows the region that the end of the beam can reach using our constant curvature



Fig. 16. Cylindrical, self-reconfiguring robot modules constructed in the Claytronics project which demonstrate rotational self-reconfiguration is possible. Each module is approximately 5 cm in diameter.

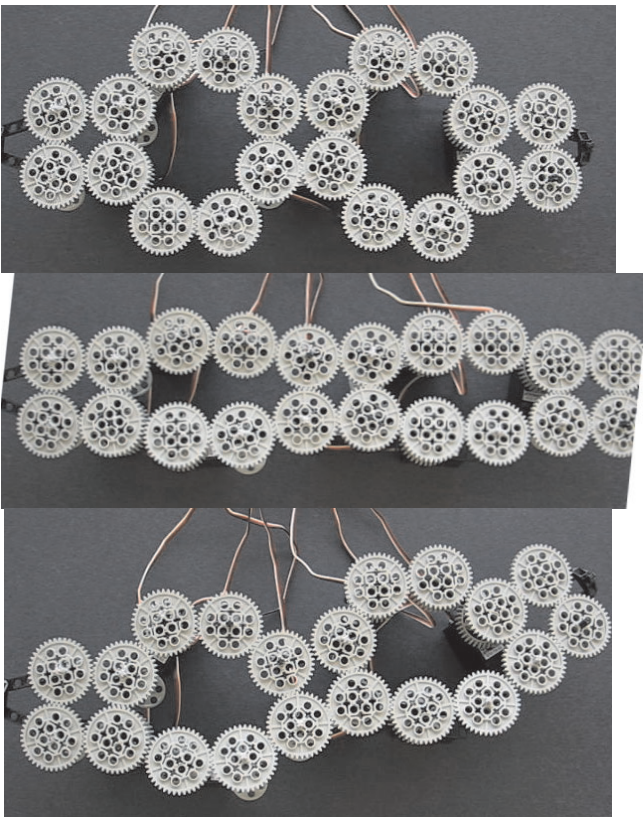


Fig. 17. Variable curvature and variable length beam similar to the simulated beam in Figure 3. This test beam uses plastic gears to represent robot modules and floating servomotors mounted under the gears to provide motive force.

control on beams consisting of 2×5 , 2×10 and 2×20 arrays of cells.

Owing to mechanical and electrical constraints this experimental apparatus drives the minimum necessary set of gear-

gear interfaces (see Figure 20), rather than all gear-gear interfaces as our simulations describe. The motive force for each cell comes from three servomotors which rotate gears 1 versus 2, 6 versus 7 and 8 versus 9 (9 is part of the adjoining cell). In addition, a pin fixes the relative orientations of gears 2 and 3, equivalent to a fourth servomotor per cell. Owing to an extra degree of freedom in the underlying system, the pinned link imposes no loss in generality. An additional, unpowered degree of freedom is set by hand at the start of experiments.

The use of toothed gears and of fixed-length, free-swinging radial links replicates “unlimited” friction between modules, an effect that could be achieved using a nanofiber adhesive on the module surfaces (Sitti and Fearing 2003), or via the shape of the modules themselves. As friction is difficult to avoid at small scales, as the module size shrinks even further, “stiction” and clumping effects might in fact require such a no-disconnection reconfiguration.

This prototype is able to smoothly transition from a short beam of roughly 85 mm wide by 245 mm long, to a narrow long structure 50 mm wide by 410 mm long. This differs from the expected change of 2:1 for the octagonal cell because we have four additional modules on the ends that do not correspond to a complete cell and because the teeth of the gears often mesh randomly on the inside of the cells as they reach their extreme configurations.

Finally, although the prototype is able to bend and straighten as in the simulations, maintaining equivalently symmetric configurations in the physical prototype has proven more difficult. Moderate but cumulative errors from the play in the mechanical interfaces and servo mountings limit the accuracy with which modules can be positioned relative to each other. This suggests that for longer structures, closed-loop monitoring of the actual resultant shape may be necessary to overcome cumulative errors along the length of the beam.

5.3. Force-test Cell

In addition to the variable aspect ratio beam above, we built a CA cell designed to test the relationship between inter-module torque and overall forces at the cell perimeter. This prototype allows us to compare the first part of our analysis from Section 3.3 with real-world data.

For this test unit we constrained a hexagonal CA cell in a jig such that only one degree of freedom remained: extension/contraction along one axis (see Figure 21). Given the jig, torque applied to modules (gears) 1, 2, 4 or 5 sufficed to drive rolling self-reconfiguration according to an actuation plan in which equal-speed, alternating-direction rotations served to expand or contract the cell along the axis joining modules 3 and 6.

With a servomotor attached to provide torque between modules 1 and 2 we applied controlled tension to module 6 along the axis joining it and module 3. We then adjusted the

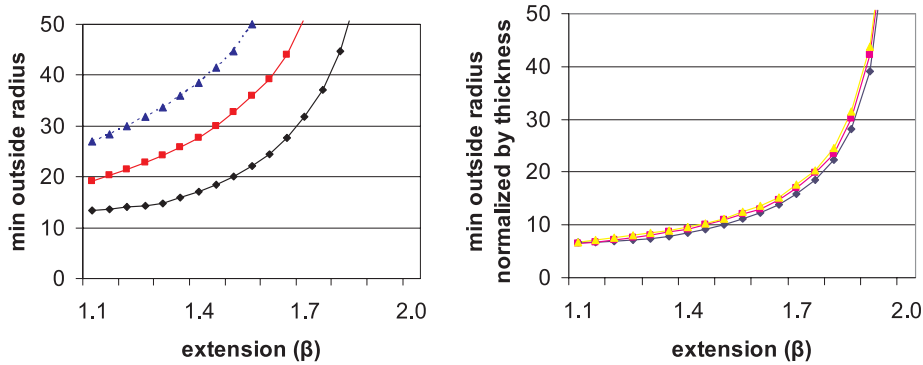


Fig. 18. (a) Tightest outside curvature achieved, as a function of inside cell extension. Plots shown for two (bottom most line), three (middle line) and four (top line) cell thick beams. (b) Normalized to beam thickness.

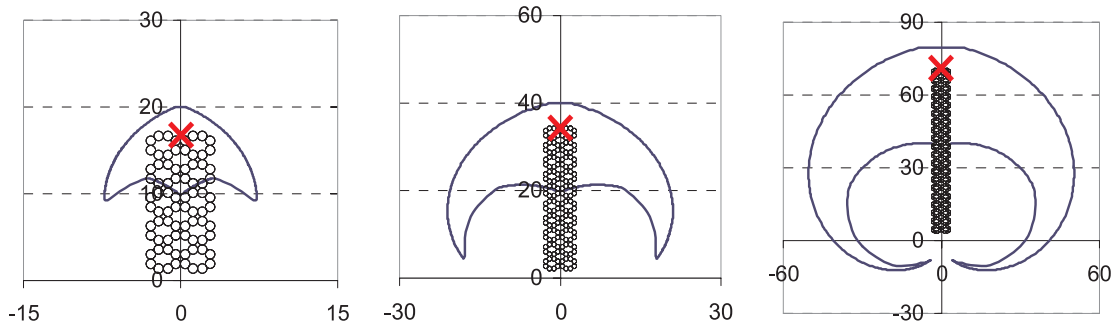


Fig. 19. Range of motion for end of beam when the other end is fixed at the origin, assuming constant curvature control. Plots correspond to beams consisting of 2×5 , 2×10 and 2×20 arrays of hexagonal cells.

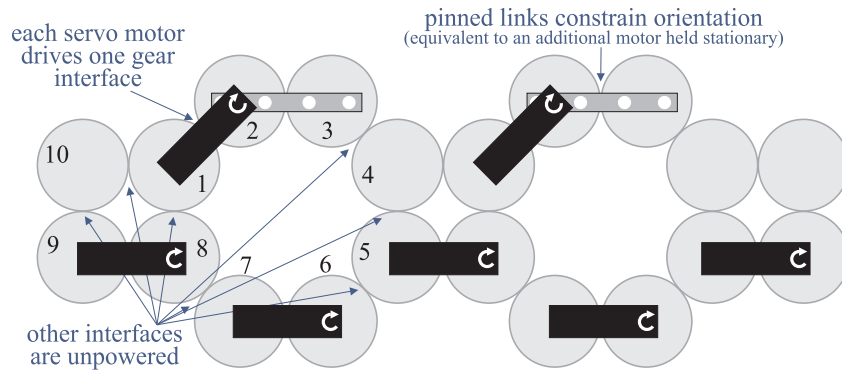


Fig. 20. Servomotor attachment points for the double-octagon prototype.

cell's position (by controlling the servo) to five different angles $\alpha \in \{49^\circ, 34^\circ, 25^\circ, 7^\circ, 2^\circ\}$. At each position we allowed the system to damp and measured the current required by the servomotor to hold the position. Figure 22 illustrates the resulting applied torque values for five objects of varying weight

across the test positions. Subsequent to the test we calibrated the servomotor by measuring its current draw under varying torque conditions.

This test is limited by the nature of its actuator (i.e. it directly controls a joint angle of the cell). Thus, it only validates

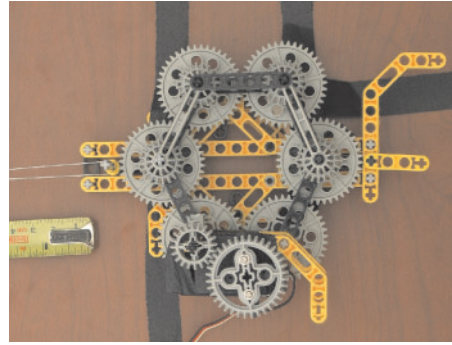
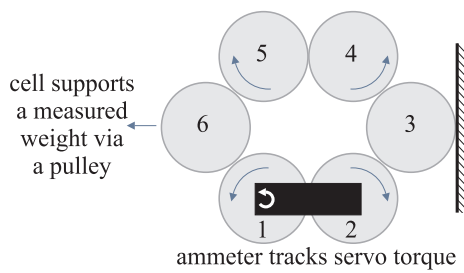


Fig. 21. Test rig for force measurements.

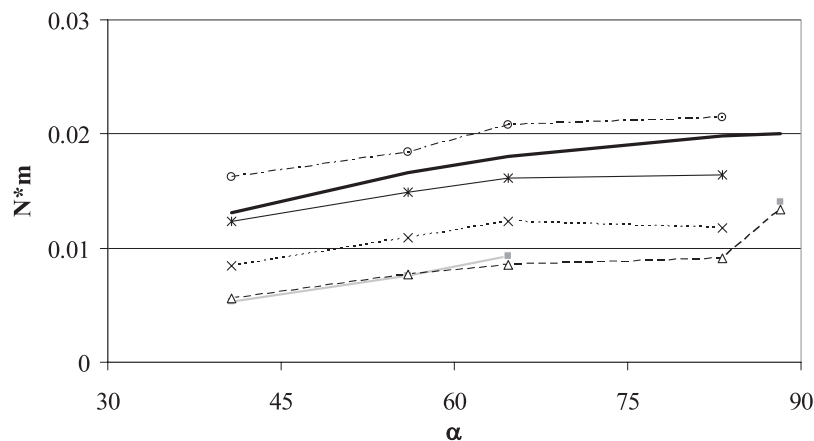


Fig. 22. Results from the force test rig. The thick black curve is an idealized force/angle curve derived from Equation (1). The remaining curves depict the holding torque required between modules (gears) 1 and 2 for five objects of varying weights.

the relationship between module perimeter (linear) velocity and angular velocity given in Equation (1), the mathematical description of a hexagonal cell and the ability of all working interfaces (including non-lifting interfaces, such as the interface equipped with a servomotor in the test rig) to contribute to moving the lifting interfaces of a cell. This test *does not* validate the full relationship derived in Sections 2.3 and 2.4 between interactor distance and cell force. We are working to build a test rig using purely action-at-a-distance actuators to validate that analysis as well.

6. Conclusion

In designing a modular robotic system, there is a clear tradeoff between high reconfigurability and increased capability, particularly with regards to actuation. This paper has described a novel technique, CA, which can use large numbers of relatively weak, but highly reconfigurable modules, in a coordinated effort to exert greater actuation forces than are possible

with individual modules. We have described how a modular ensemble technique based on collections of CA cells can facilitate the construction of much larger structures by stacking multiple cells together. Owing to the potential for hierarchical decomposition, even very large ensembles can be directed with relatively low control complexity.

We have presented a variety of analyses based on theory and simulations as well as empirical results from several physical experiments on prototype CA cells. Taken together these results strongly support our thesis that CA techniques can exert forces significantly larger than a single pair of modules can.

This paper has focused on the actuation mechanics of cylindrical or spherical modules, treated as a single machine with rotating parts and infinite traction between modules. Future work will consider the effects of limited inter-module friction, control strategies that may be necessary to maintain structural integrity and the impact of coordination errors and hardware and software failures. We will also study dynamic reconfiguration to ensure parallel groups of actuating cells are kept in a configuration of maximal mechanical advantage.

References

- Campbell, J. and Pillai, P. (2006). Collective actuation. *Proceedings of the Robotics Science and Systems: Workshop on Self-Reconfigurable Modular Robots*.
- Christensen, D. J., Brandt, D. and Støy, K. (2006). Towards artificial ATRON animals: scalable anatomy for self-reconfigurable robots. *Proceedings of the Robotics Science and Systems: Workshop on Self-Reconfigurable Modular Robots*.
- De Rosa, M. and Goldstein, S. C. and Lee, P. and Campbell, Jason and Pillai, Padmanabhan. (2006). Scalable Shape Sculpting via Hole Motion. *Proceedings of the IEEE International Conference on Robotics and Automation (ICRA)*.
- Goldstein, S. C., Campbell, J. and Mowry, T. C. (2005). Exploring programmable matter. *IEEE Computer*, **38**(6): 99–101.
- Gough, V. E. (1956). Contribution to discussion of papers on research in automobile stability, control and tyre performance. *Proceedings of the Automotive Division of the Institution of Mechanical Engineers*, pp. 392–394.
- Jorgensen, M. W., Ostergaard, E. H. and Lund, H. H. (2004). Modular Atron: modules for a self-reconfigurable robot. *Proceedings of the IEEE International Conference on Intelligent Robots and Systems (IROS)*.
- Kieffer, J. and Lenarcic, J. (1994). On the exploitation of mechanical advantage near robot singularities. *Informatica*, **18**(3): 315–323.
- Kirby, B., Campbell, J., Aksak, B., Pillai, P. S., Hoburg, J., Mowry, T. C. and Goldstein, S. C. (2005). Catoms: moving robots without moving parts. *Proceedings of AAAI (Demo Abstracts)*.
- Lenhart, W. J. and Whitesides S. H. (1994). Reconfiguring simple polygons. *Discrete and Computational Geometry*.
- Luntz, J. E. and Messner, W. (1995). Work on a highly distributed coordination control system. *Proceedings of the AACC American Controls Conference*.
- Murata, S., Kurokawa, H. and Kokaji, S. (1994). Self-assembling machine. *Proceedings of the IEEE International Conference on Robotics and Automation (ICRA)*, pp. 441–448.
- Murata, S., Yoshida, E., Kamimura, A., Kurokawa, H., Tomita, K. and Kokaji, S. (2002). M-tran: self-reconfigurable modular robotic system. *IEEE/ASME Transactions on Mechatronics*, **7**(4): 431–441.
- Rus, D. and Vona, M. (1999). Self-reconfiguration planning with compressible unit modules. *Proceedings of the IEEE International Conference on Robotics and Automation (ICRA)*.
- Sitti, M. and Fearing, R. (2003). Synthetic gecko foot-hair micro/nano-structures as dry adhesives. *Journal of Adhesion Science and Technology*, **17**(8): 1055–1074.
- Suh, J., Homans, S. B. and Yim, M. (2002). Telecubes: mechanical design of a module for a self-reconfigurable robotics. *Proceedings of the IEEE International Conference on Robotics and Automation (ICRA)*, pp. 4095–4101.
- Trinkle, J. C. and Milgram, R. J. (2002). Complete path planning for closed kinematic chains with spherical joints. *International Journal of Robotics Research*, **21**(9): 773–789.
- Vassilvitskii, S., Kubica, J., Rieffel, E., Yim, M. H. and Suh, J. W. (2002a). On the general reconfiguration problem for expanding cube style modular robots. *Proceedings of the IEEE International Conference on Robotics and Automation (ICRA)*.
- Vassilvitskii, S., Suh, J. and Yim, M. (2002b). A complete, local and parallel reconfiguration algorithm for cube style modular robots. *Proceedings of the IEEE International Conference on Robotics and Automation (ICRA)*.
- Yim, M. (1993). A reconfigurable modular robot with many modes of locomotion. *Proceedings of the JSME International Conference on Advanced Mechatronics*.
- Yim, M. (1994). Locomotion with a unit modular reconfigurable robot. *Ph.D. Thesis*, Stanford University, Department of Mechanical Engineering.
- Yim, M., Duff, D. and Roufas, K. (2000). Polybot: a modular reconfigurable robot. *Proceedings of the IEEE International Conference on Robotics and Automation (ICRA)*, pp. 514–520.
- Yim, M., Duff, D. and Zhang, Y. (2001). Closed-chain motion with large mechanical advantage. *Proceedings of the IEEE International Conference on Intelligent Robots and Systems (IROS)*.
- Yim, M., Reich, J. and Berlin, A. (2000). Two approaches to distributed manipulation. *Distributed Manipulation*, Choset, H. and Bohringer, K. (eds). Dordrecht, Kluwer.